AMERICAN SOCIETY FOR MICROBIOLOGY | Molecular and Cellular Biology

Phosphorylation of Ago2 and Subsequent Inactivation of let-7a RNP-Specific MicroRNAs Control Differentiation of Mammalian Sympathetic Neurons

Somi Patranabis, Suvendra Nath Bhattacharyya

RNA Biology Research Laboratory, Molecular Genetics Division, CSIR-Indian Institute of Chemical Biology, Kolkata, India

MicroRNAs (miRNAs) are small regulatory RNAs that regulate gene expression posttranscriptionally by base pairing to the target mRNAs in animal cells. *KRas*, an oncogene known to be repressed by let-7a miRNAs, is expressed and needed for the differentiation of mammalian sympathetic neurons and PC12 cells. We documented a loss of let-7a activity during this differentiation process without any significant change in the cellular level of let-7a miRNA. However, the level of Ago2, an essential component that is associated with miRNAs to form RNP-specific miRNA (miRNP) complexes, shows an increase with neuronal differentiation. In this study, differentiation-induced phosphorylation and the subsequent loss of miRNA from Ago2 were noted, and these accounted for the loss of miRNA activity in differentiating neurons. Neuronal differentiation induces the phosphorylation of mitogen-activated protein kinase p38 and the downstream kinase mitogen- and stress-activated protein kinase 1 (MSK1). This in turn upregulates the phosphorylation of Ago2 and ensures the dissociation of miRNA from Ago2 in neuronal cells. MSK1-mediated miRNP inactivation is a prerequisite for the differentiation of neuronal cells, where let-7a miRNA gets unloaded from Ago2 to ensure the upregulation of *KRas*, a target of let-7a. We noted that the inactivation of let-7a is both necessary and sufficient for the differentiation of sympathetic neurons.

PC12 cells derived from the pheochromocytoma of the rat adrenal medulla are widely used for studying cell signaling in response to numerous growth factors, neurotrophins, and hormones. These cells serve as a useful model to study the proliferation, differentiation, and survival of sympathetic neurons (1). PC12 cells stop dividing and differentiate to cells with neuronal extensions when cultured in the presence of nerve growth factor (NGF) and low levels of serum (2). Differentiated PC12 cells show changes in their electrical excitability, sensitivity to acetylcholine, and choline acetyltransferase activity (3). NGF-, brain-derived neurotrophic factor (BDNF)-, or cyclic AMP-treated, differentiated PC12 cells are connected to each other, although it is not clear whether newly formed neuronal extensions or neurites form functional synapses or not (4). The paradoxical finding that the *Src* and *Ras* oncogene products enhanced rather than blocked NGF-induced differentiation led to the identification of signaling pathways involving both Ras and Src as part of the total differentiation response to NGF (5). In PC12 cells, Ras accounts for the immediate effects of NGF, mediated through extracellular signal-regulated kinase (ERK) (1).

MicroRNAs (miRNAs), a class of 21-nucleotide-long noncoding RNAs, can reversibly repress the translation of their target messages by binding the mRNA with imperfect complementarities in metazoan cells. miRNA-targeted messages and the components of the miRNA machinery, including the Argonaute (Ago) proteins and miRNAs, accumulate in mammalian P bodies (6–8). miRNAs can control neuronal differentiation (9). Determination of the temporal expression patterns of 138 miRNAs in mouse brain revealed changes in the expression of 66 miRNAs during neuronal development (10). miRNA-9 (miR-9) controls the differentiation of embryonic stem cells to neurons (11), whereas miR-124a, a well-conserved abundant miRNA expressed throughout the embryonic and adult central nervous system, plays an important role in neuronal differentiation and synaptic function (12, 13). Fragile mental retardation protein (FMRP)-associated miR-125b stimulates the dendritic branching of neurons (14), whereas miR-132 enhances dendritic complexity (15) and miR-128 increases dendritic growth (16).

Ago proteins play a major role in the regulation of miRNAs. They are crucial in determining small RNA-dependent gene silencing in eukaryotes. Recent reports suggest that in mammalian cells, Argonaute proteins regulate the expression of the majority of protein-encoding genes through posttranscriptional mechanisms (17). Posttranslational modification of Argonaute proteins can modulate RNA-induced silencing complex (RISC) formation and/or activity. Modifications like hydroxylation or methylation are known to increase Argonaute stability and, consequently, gene silencing functions (18, 19). Many eukaryotic proteins are regulated by different protein kinases. Like many such proteins in eukaryotic cells, Argonaute proteins are also the substrates for multiple protein kinases (20–23). There are four members of the Ago subfamily in mammalian cells, but of these members, Ago2 is the most widely expressed and predominant Argonaute isoform in mammalian somatic cells and the only member that can cleave targeted mRNAs (24).

Of the different posttranslational modifications, Argonaute phosphorylation is known to affect small RNA-based gene silenc-

Received 21 January 2016 **Accepted** 30 January 2016

Accepted manuscript posted online 8 February 2016

Citation Patranabis S, Bhattacharyya SN. 2016. Phosphorylation of Ago2 and subsequent inactivation of let-7a RNP-specific microRNAs control differentiation of mammalian sympathetic neurons. Mol Cell Biol 36:1260–1271. doi:10.1128/MCB.00054-16.

Address correspondence to Suvendra Nath Bhattacharyya, suvendra@iicb.res.in.

ing through multiple mechanisms (25). One such example is the phosphorylation of tyrosine-393, which negatively impacts the interaction between Ago2 and Dicer, which in turn affects miRNA maturation (22). Once pre-miRNAs are processed into mature duplexes, the middle (MID) domains of Argonaute proteins anchor the 5′ phosphates of guide RNA strands in RISC. On the other hand, loading of small RNAs onto RISC is prevented by the phosphorylation of tyrosine-529 in this domain of Ago2 (21). This indicates that the regulated phosphorylation of tyrosine-529 may be a critical step in RISC activation. In addition, the endonucleolytic cleavage activity of Ago2 is reported to be suppressed by the phosphorylation status of serine-387, while it enhances the silencing of the targeted mRNAs by translational repression (20). The phosphorylation of serine-387 reportedly stimulates Ago2 interaction with GW182, a P-body-resident protein and critical component of the ribonucleoprotein (RNP) complex, and this increased interaction between phosphorylated Ago2 and GW182 may underlie the change of the silencing mechanism for this protein. Therefore, the phosphorylation of serine-387, tyrosine-393, and tyrosine-529 regulates Argonaute activity by three different mechanisms (25).

A specific tyrosine residue, Y529, in human Ago2, located in the small RNA 5′-end-binding pocket of the MID domain, has some degree of predicted surface availability, and increasing evidence indicates that it is phosphorylated *in vivo* (21, 26). By structural modeling and a number of biochemical approaches, it was found that placement of a negative charge in the position of the tyrosine side chain interferes with the binding of the 5′ phosphate of the small RNA. The phosphotyrosine sterically hinders the docking of a second phosphate, and the negative charge generates a repulsive force against another negatively charged group. Thus, the phosphorylation of the highly conserved Y529 within the 5′-end-binding pocket of the MID domain of Ago2 might function as a molecular switch that promotes or inhibits small RNA binding to Argonaute proteins (21). A recent report indicates that a transient reversal of miRNA-mediated repression occurs through Ago2 phosphorylation and that this results in impaired binding of Ago2 to miRNAs and to the corresponding target mRNAs during the early phase of the inflammatory response in macrophages (26).

In the study described in this report, the regulation of miRNA activity by neuronal differentiation in mammalian cells was investigated. We found that the reduced activity of let-7a miRNA due to the phosphorylation-driven inactivation of existing RNP-specific miRNAs (miRNPs) results in increased expression of the KRas protein, augments the p38 signaling pathway in rat sympathetic neurons, and is both necessary and sufficient for the differentiation of sympathetic neurons.

MATERIALS AND METHODS

Cell culture. Rat pheochromocytoma (PC12) cells were cultured in Dulbecco's modified Eagle's medium (DMEM; Gibco) supplemented with 2 mM L-glutamine, 10% heat-inactivated horse serum (HS), and 5% heat-inactivated fetal bovine serum (FBS). Cells were differentiated in medium containing DMEM supplemented with 0.25% heat-inactivated FBS, 0.75% heat-inactivated HS, and 100 ng/ml nerve growth factor (Promega). SB203580, a p38 mitogen-activated protein kinase (MAPK) inhibitor, was used at a concentration of 10 μM and was added to the cell culture medium overnight to inhibit p38 MAPK in PC12 cells (27).

Primary culture. Neonatal Sprague-Dawley rat pups (age, postpartum day 0 [P0] or P1) were collected. They were rapidly decapitated under sterile conditions. The superior cervical ganglia were isolated from each pup, and a primary sympathetic neuron culture was established according to an established protocol (28).

Ethics statement. The use of rat pups was approved by the Institutional Animal Ethics Committee of CSIR-Indian Institute of Chemical Biology, Kolkata, India. All the experimentations were performed according to the national regulatory guidelines issued by the Committee for the Purpose of Supervision of Experiments on Animals, Ministry of Environment and Forest, Government of India. All the experiments involving animals were carried out with prior approval of the institutional animal ethics committee.

Plasmid constructs. Plasmids containing a humanized renilla luciferase (RL) coding region (pRL-Con), three let-7a binding sites (pRL-3×Bulge-let-7a), and a perfect let-7a binding site (pRL-Perfect) downstream of the RL-coding region were kind gifts from Witold Filipowicz. A plasmid expressing firefly luciferase (FL) under the control of a simian virus 40 promoter (PGL3-FF) was from Promega. Plasmid RL HMGA2-3′UTR containing 3 kb of the wild-type 3′ untranslated region (UTR) of the *HMGA2* gene with intact miRNA binding sites cloned downstream of the pRL-Con plasmid was from Anindya Dutta. Plasmid FLAG-HA-Ago2, expressing FLAG- and hemagglutinin (HA)-tagged human AGO2, along with its mutants, FLAG-HA-AGO2 Y529E (phosphor dead) and FLAG-HA-AGO2 Y529F (phosphor mimetic), expressing FLAG- and HA-tagged human AGO2 with a mutation from tyrosine to glutamic acid and phenylalanine at position 529, respectively, was obtained from Gunter Meister. Plasmid FLAG-HA-Ago2 stably expressing FLAG- and HA-tagged human AGO2 in HEK293 cells was received from Tom Tuschl. A plasmid expressing the pre-let-7a and the let7-a coding region, which was amplified and cloned in the pCIneo vector (pCIneo-let-7a), was generated as described by J. G. Belasco. Construction of a plasmid encoding pre-miR-122 under the control of a constitutive U6 promoter, pmiR-122, was described by J. Chang. Sense and antisense primers specific for small interfering RNA (siRNA) against RL (siRL) were synthesized with Eurogentec, and si AllStars negative-control siRNA was purchased from Qiagen.

Cell transfection. To express HA-tagged Ago2 and its mutants, cells were transfected with 1 μg expression plasmid DNA in a 12-well format. For the luciferase assay, cells were transfected with 20 ng of a plasmid expressing RL and 200 ng of a plasmid expressing FL in a 24-well format. Anti-let-7a, anti-miR-122 (Ambion), and siRNAs were transfected at a 100 nM concentration. ON-TARGETplus SMARTpool siRNA against mitogen- and stress-activated protein kinase 1 (MSK1) was obtained from Dharmacon. PC12 cells were transfected using the Lipofectamine LTX reagent (Invitrogen). The Fugene HD reagent (Roche) was used as the transfection reagent for primary neurons. All transfections were done following the manufacturers' protocols.

Luciferase assay. RL and FL activities were measured using a dual-luciferase assay kit (Promega) following the supplier's protocol on a Victor X3 plate reader with injectors (PerkinElmer). Before the luciferase activity was measured, cells were lysed with 1× passive lysis buffer (Promega). FL-normalized RL expression levels for the reporter and the control were used to calculate the fold repression.

Western blotting. After cell lysis, quantification was done using the Bradford reagent (Thermo Scientific). A stipulated amount of the sample was diluted in 5× sample loading buffer (312.5 mM Tris-HCl, pH 6.8, 10% SDS, 50% glycerol, 250 mM dithiothreitol [DTT], 0.5% bromophenol blue) and heated for 10 min at 95°C. Following SDS-polyacrylamide gel electrophoresis of the extracts, proteins were transferred to a polyvinylidene difluoride membrane (Millipore). The membranes were blocked in Tris-buffered saline (TBS) containing 0.1% Tween 20 and 3% bovine serum albumin (BSA). Primary antibodies in 3% BSA were added for a minimum of 16 h at 4°C, followed by washing of the membranes at room temperature thrice for 5 min each time with TBS containing 0.1% Tween 20, and the membranes were incubated at room temperature for 1 h with secondary antibodies conjugated with horseradish peroxidase (1:8,000

dilution). Excess antibodies were washed three times with TBS–Tween 20 at room temperature. Signals were detected with the West chemiluminescent substrate using the manufacturer's protocol (Thermo-Scientific). Imaging of all Western blots was performed using a UVP Bio-Imager 600 system equipped with VisionWorks Life Science software (v6.80; UVP). Bands were quantified using QuantOne software. Antibody against HRS was obtained from Bethyl; phosphotyrosine-specific antibody 4G10 and antibody against phosphoserine were obtained from Millipore; antibodies against HA, KRas, and β-actin were obtained from Roche; antibody against Alix and GAP43 were obtained from Santa Cruz; Ago2 (EIF2C2) antibody was obtained from Novus Biologicals; and antibodies against calnexin, LAMP1, MSK1, phospho-p38, phospho-mTOR, and phospho-MSK1 (p-MSK1) were obtained from Cell Signaling.

IP and cell fractionation. Cell fractionation using OptiPrep density gradient centrifugation was carried out as described previously (26). For immunoprecipitation (IP) reactions, cells (transfected in the case of tagged proteins) were lysed in 1× lysis buffer (20 mM Tris-HCl, pH 7.5, 150 mM KCl, 5 mM $MgCl_2$, and 1 mM DTT with 1% Triton X-100, 40 U/ml RNase inhibitor [Fermentas], and 1× EDTA-free protease inhibitor cocktail [Roche]) for 30 min at 4°C. The lysates were clarified by centrifugation, followed by incubation with antibody-bound recombinant protein G-agarose beads, obtained by preincubation of antibody to the recombinant protein G-agarose beads (Invitrogen) for 4 h at 4°C on a rotator. The beads were initially blocked with 5% BSA in 1× lysis buffer. For immunoprecipitation of FLAG-tagged proteins, lysate was incubated with anti-FLAG M2-agarose antibody (Sigma). After that, the beads were washed thrice with IP buffer (20 mM Tris-HCl, pH 7.5, 150 mM KCl, 5 mM $MgCl_2$, 1 mM DTT), and the beads were separated into two parts. One-half of the beads were boiled at 95°C for 10 min, centrifuged at 13,000 × *g*, and used for protein estimation, and the other half of the beads were used for RNA extraction.

***In vitro* kinase assay.** FLAG-HA-Ago2 was immunoprecipitated from FLAG-HA-Ago2 stable HEK293 cells using FLAG-tagged beads and then eluted from the bead with FLAG peptide in the presence of elution buffer. Phospho-MSK1 was immunoprecipitated from naive and differentiated PC12 cells, and the beads were incubated with the eluates for 30 min at 37°C in the presence of 1 mM ATP. The reaction mix was centrifuged at 13,000 × *g* for 2 min, and the supernatant was used for Western blotting.

RNA isolation and quantification. Total RNA was isolated by using the TRIzol reagent (Invitrogen) according to the manufacturer's protocol. One-step reverse transcription (RT)-PCR was done with specific primers and by following the manufacturer's protocol (Invitrogen). For quantitative RT-PCR of miRNAs, the let-7a, let-7b, let-7e, miR-122, miR-9, miR-128a, and U6 levels were quantified with a TaqMan-based miRNA assay kit (Applied Biosystems) following the manufacturer's instructions, while let-7f, RL, RL3XB, and 18S rRNA levels were quantified with target-specific primers using a SYBR green-based RT-PCR detection kit (Eurogentec) following the manufacturer's instruction. One hundred nanograms of total RNA was used for miRNA quantification in the RT reaction. The RT reaction mixture was diluted twice in water, and equal volumes of aliquots were subsequently used for amplification according to the manufacturer's instructions (Applied Biosystems). The RT reaction conditions were 16°C for 30 min, 42°C for 30 min, and 85°C for 5 min, and the mixture was then held at 4°C. The PCR conditions were 95°C for 5 min, 95°C for 15 s, and 60°C for 1 min for 40 cycles.

Northern blotting of miRNA. For detection by Northern blotting, RNA was extracted by using the TRIzol reagent according to the manufacturer's protocol (Invitrogen). A designated amount of total RNA was separated on a 15% urea–polyacrylamide gel, which was transferred to an Immobilon Nylon+ membrane (Millipore). The RNA was cross-linked to the membrane with UV radiation. Hybridization was carried out by a standard protocol. The probe sequence was complementary to the mature form of the miRNA of interest and was labeled with γ-^{32}P. After being washed, the membranes were imaged by using a phosphorimager (PerkinElmer).

Immunofluorescence. Cells on coverslips were fixed using 4% paraformaldehyde in phosphate-buffered saline (PBS) in the dark at room temperature for 30 min. Coverslips were washed thrice with 1× PBS, blocked, and permeabilized using 1× PBS containing 10% goat serum (Gibco), 1% bovine serum albumin (Affymetrix; USB), and 0.1% Triton X-100 (Calbiochem) for 30 min at room temperature. Primary antibody, diluted in 1× PBS with 1% BSA, was added to cells on coverslips at 4°C overnight in a humid chamber, followed by three washes with 1× PBS for 5 min each time. Alexa Fluor-labeled secondary antibody (1:500; Invitrogen), diluted in 1× PBS with 1% BSA, was added to cells on coverslips. The coverslips were placed in a humid chamber at room temperature for 1 h, and the cells were washed three times with 1× PBS for 5 min each and mounted with Vectashield mounting medium with DAPI (4′,6-diamidino-2-phenylindole; Vector).

Image capture and postcapture image processing. Cells were imaged with an inverted Eclipse Ti Nikon microscope equipped with a Plan Apo VC 60× oil objective (numerical aperture, 1.40) and a Nikon Qi1MC camera for image capture. z-stack images were captured with am IXON3 electron-multiplying charge-coupled-device camera. All images captured on the Nikon Eclipse Ti microscope were deconvoluted, analyzed, and processed with Nikon NIS Element AR (v3.1) software.

Statistical analysis. All graphs and statistical analyses were generated in Prism (v5.00) software (GraphPad, San Diego, CA). Nonparametric unpaired and paired *t* tests were used for analysis. *P* values of <0.05 were considered statistically significant, and *P* values of >0.05 were not significant. Error bars indicate means ± standard deviations (SDs).

RESULTS

Increased expression of *KRas* and decreased let-7a miRNA activity during NGF-induced differentiation of rat sympathetic neurons and PC12 cells. *KRas* is an oncogene that is involved in NGF-induced PC12 cell differentiation (1). It was observed that with an increasing time of treatment with NGF, there was a gradual increase in the level of the KRas protein (Fig. 1A). The level of *KRas* mRNA in undifferentiated cells and cells that had been differentiated for 72 h was also checked, and an increase in the mRNA level in differentiated cells was noted (Fig. 1B). KRas is a let-7a miRNA-regulated molecule (29). Thus, we were interested to determine the effect of differentiation on let-7a. Interestingly, the activity of let-7a miRNA dropped significantly upon differentiation of PC12 cells without a change in the mature let-7a miRNA level (Fig. 1C to E). Not only was the activity decrease true for let-7a miRNA, but a similar decrease in the activity of exogenously expressed miR-122 was also noted in differentiating PC12 cells (Fig. 1E). A decrease in let-7a activity without a change in the mature let-7a level was also observed in rat primary sympathetic neurons with the progression of differentiation *ex vivo* (Fig. 1F and G). Since the Ago2 protein is the other major constituent of miRNPs, a reduction in the level of Ago2 could account for the reduced miRNA activity in differentiated PC12 cells. Unlike the expected result, however, with differentiation we noted the increased expression of Ago2 at both the mRNA and protein levels (Fig. 1H and I). A similar increase in the expression of Ago2 was also documented in NGF-treated rat primary neurons obtained from the superior cervical ganglion (SCG) (Fig. 1J and K). In each case, the differentiation status of the cells after NGF treatment was confirmed by the enhanced expression of GAP43 at both the mRNA and protein levels.

The decreased activity of miRNA in differentiated PC12 cells is caused by the loss of miRNA from phosphorylated Ago2. To test whether a reduction in the level of miRNPs in differentiated neuronal cells could account for the reduced miRNA activity, we

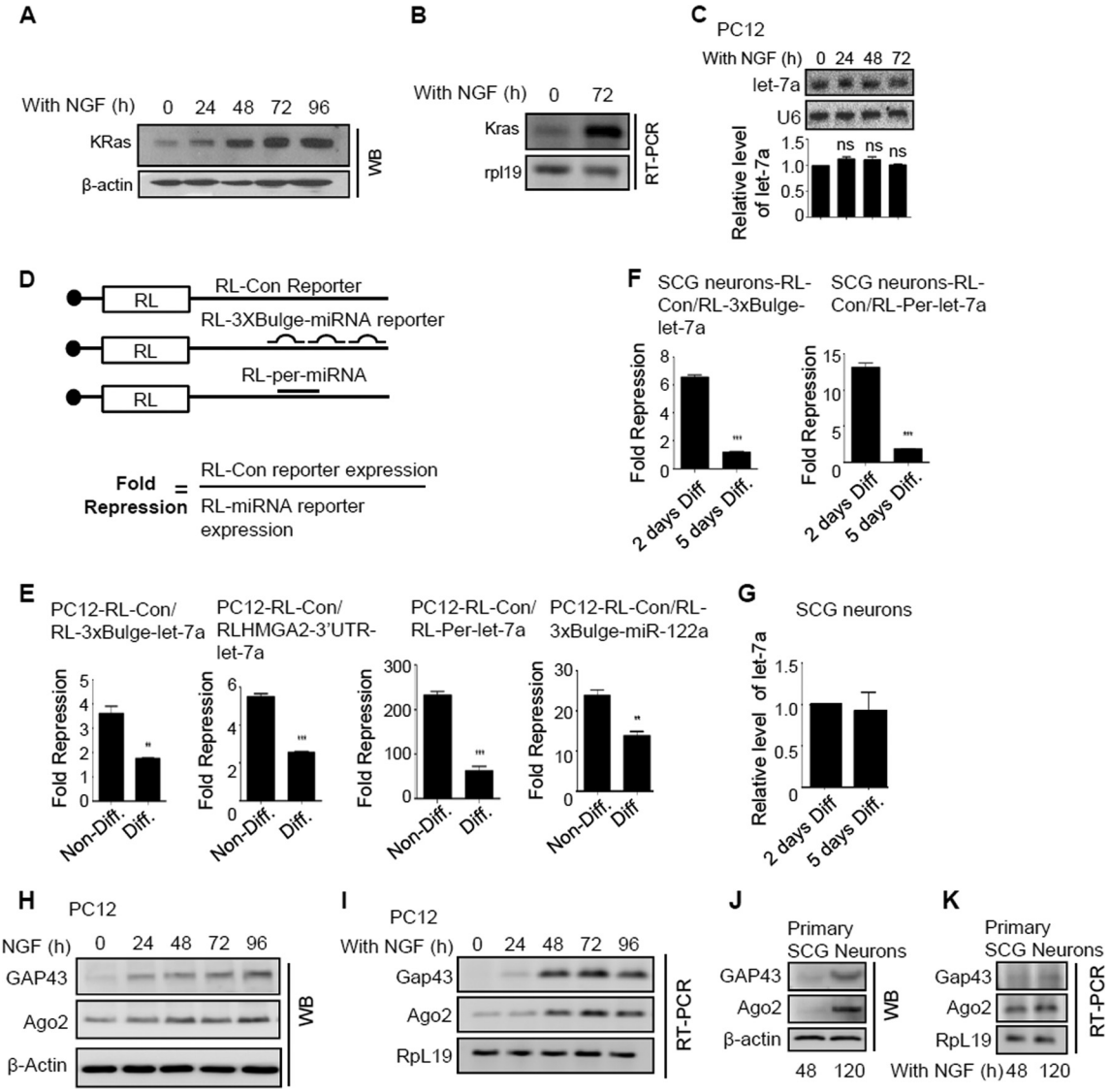

FIG 1 Upregulation of *KRas* and loss of let-7a activity with neuronal differentiation. (A) Expression of KRas with increasing time of differentiation in PC12 cells was checked by Western blotting (WB) using β-actin as a loading control. (B) RT-PCR of undifferentiated and differentiated PC12 cells to check the Ras level using Rpl19 as a loading control. (C) (Top) Northern blotting detection of miRNA let-7a and U6 in naive PC12 cells and NGF-differentiated PC12 cells. U6 snRNA was used as a loading control. (Bottom) The intensities of the signals in the blots were quantified, and the relative level of let-7a was plotted. (D) Schematic representation of luciferase reporters showing the respective miRNA binding sites. (E) Fold repression of miRNA reporters with either one perfect let-7a miRNA binding site or multiple bulged let-7a miRNA binding sites in undifferentiated (Non-Diff.) and differentiated (Diff.) PC12 cells. The reporter RLHMGA2 contains the 3′ UTR of the *HMGA2* gene, an endogenous let-7a target. RL mRNA with no let-7a binding sites in the 3′ UTR was used as a control. For the miR-122 activity assay, PC12 cells exogenously expressing miR-122 by transfection of phosphorylated miR-122 were used. (F) Decrease in let-7a activity in rat SCG primary neurons upon differentiation with NGF. The fold repression of let-7a miRNA reporters with multiple imperfect sites or one perfect let-7a site was measured and plotted. (G) Real-time PCR-based quantification to estimate the changes in the level of let-7a miRNA with differentiation of SCG primary neurons. U6 snRNA was used as a loading control. (H to K) Expression of Ago2 in PC12 cells differentiated by NGF treatment (H, I) or in rat primary neurons (J, K) was checked. Western blotting-based (H, J) and RT-PCR-based (I, K) assays were used to estimate the expression of the neuronal differentiation marker gene *GAP43* and the Ago2 protein in undifferentiated and differentiated PC12 cells and in rat primary neurons. β-Actin and Rpl19 were used as loading controls. The data are from four biological replicates and represent means ± SEMs. ns, nonsignificant; *, $P < 0.05$; **, $P < 0.001$; ***, $P < 0.0001$.

immunoprecipitated Ago2 and measured the amount of miRNA present with each unit of immunoprecipitated Ago2. We detected a reduction in the amount of miRNAs bound to Ago2 in differentiated PC12 cells, which could account for the low let-7a activity in differentiated PC12 cells (Fig. 2A). The phosphorylation of Ago2 can cause the deregulation of miRNA binding to Ago2 (21). Ago2 phosphorylated at Tyr-529 showed reduced miRNA binding both *in vivo* and *in vitro*. The increased phosphorylation of immunoprecipitated Ago2 was detected with a phosphotyrosine-specific antibody (Fig. 2B). Differentiated PC12 cells showed an increase in phosphorylation level compared to undifferentiated PC12 cells. The increased Ago2 phosphorylation correlates with the reduced miRNA binding of Ago2 immunologically isolated from differentiated PC12 cells. This phenomenon was also observed *in vivo*

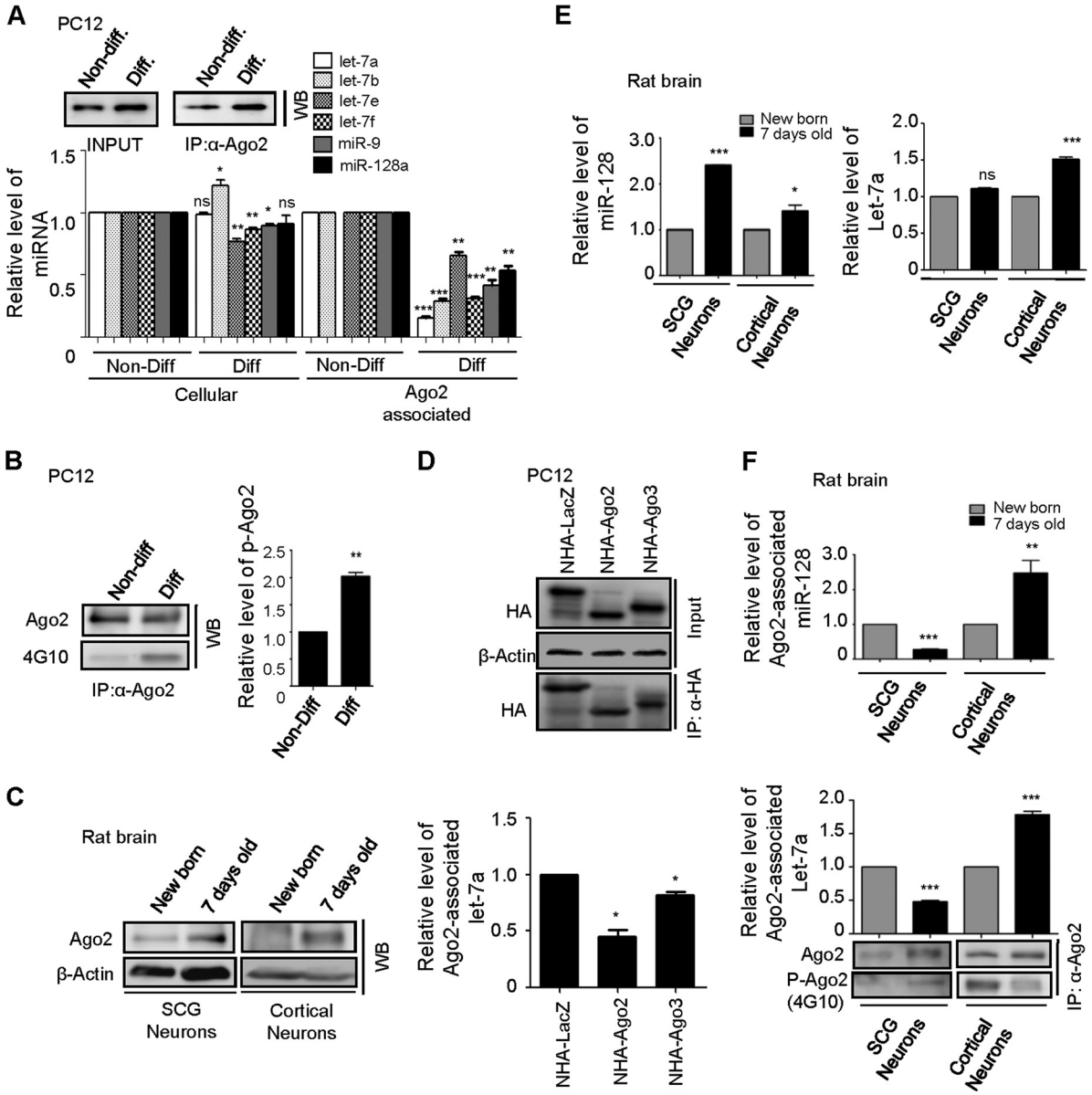

FIG 2 The loss of miRNA binding to Ago2 during differentiation of sympathetic neurons causes a reduction of miRNA activity in differentiated cells. (A) Loss of miRNAs from immunoprecipitated Ago2 isolated from NGF-differentiated PC12 cells. The relative levels of the miRNAs in total and Ago2-immunoprecipitated RNAs were estimated by real-time RT-PCR, and Ago2 was detected by Western blot analysis. (B) Increased phosphorylation of Ago2 in differentiating PC12 cells. (Left) The phosphorylated form of Ago2 (p-Ago2) was detected with a phosphotyrosine-specific antibody (4G10) in affinity-purified Ago2 materials isolated from naive and differentiated PC12 cell extracts. (Right) Relative levels of phosphorylated Ago2 in naive and differentiated PC12 cells. (C) Western blotting was done to determine the Ago2 expression level in the sympathetic and cortical regions of newborn and 7-day-old rat pup brains. (D) (Top) Western blots indicate the input and HA-immunoprecipitated levels of NHA-LacZ (control), NHA-Ago2, and NHA-Ago3 (fusion proteins with viral N peptide and hemagglutinin [HA] epitopes at their N termini). (Bottom) NHA-Ago2- and NHA-Ago3-associated let-7a miRNA levels, along with NHA-LacZ-associated let-7a miRNA levels as a control, in PC12 cells. (E) Levels of miR-128a (left) and let-7a (right) in total RNA isolated from the SCG and cortical regions of rat brain were estimated. (F) Relative amounts of miR-128a (top) and let-7a (middle) associated with endogenous Ago2 in the sympathetic and cortical regions of newborn and 7-day-old rat pup brains. (Bottom) Western blotting indicates the amount of immunoprecipitated Ago2 or its phosphorylated form in the sympathetic and cortical regions of newborn and 7-day-old rat pup brains. The data are from three biological replicates for PC12 cells and four biological replicates for rat pups. The relative level of phosphorylated Ago2 is shown. Data represent means ± SEMs. ns, nonsignificant; *, $P < 0.05$; **, $P < 0.001$; ***, $P < 0.0001$.

during the differentiation of neurons in rat brain. Ago2 expression also increased with time both in the brain cortex and in the SCG (Fig. 2C). Interestingly, human Ago3, which lacks a Tyr at position 529, did not show any significant loss of miRNA binding compared to that of the Ago2 protein (Fig. 2D). Although the total level of miR-128a, a neuronal miRNA, increased both in the SCG and in the cortical regions of brain, the total let-7a level remained unchanged in the SCG region but increased in the cortical region of the brains of 7-day-old rat pups compared to the total let-7a level in the cortical region of the brains of newborn rat pups (Fig. 2E). The level of association of let-7a and miR-128a with immunoprecipitated Ago2 decreased in the SCG region and increased in

the cortical region of the brains of 7-day-old rat pups compared to the level of association found in the brains of newborn rat pups. Consistent with the phosphorylation-related reduction of Ago2 binding of miRNA in rat brain, the levels of Ago2 phosphorylation were higher in the SCG region but were lower in the cortical region of the brains of 7-day-old rat pups in comparison to the levels of phosphorylation found in the brains of newborn rat pups (Fig. 2F).

Phosphorylation of Ago2 is necessary for neuronal differentiation. The Tyr at position 529 of Ago2 has previously been shown to play a major role in the miRNA binding of Ago2 (21). Immunofluorescence data obtained with phosphor-dead and phosphor-mimetic mutants of Ago2 along with a wild-type variant of Ago2 indicated that expression of phosphor-mimetic (Y529E) and wild-type Ago2 leads to increased PC12 differentiation, as indicated by the increase in the lengths of neurites compared to the lengths of the neurites in PC12 cells with the phosphor-dead (Y529F) variant of Ago2 (Fig. 3A and B). Consistent with the increased phosphorylation and the increased level of Ago2 in differentiated PC12 cells, incubation of immunoprecipitated FLAG-tagged Ago2 with the lysate of differentiated PC12 cells led to the preferential degradation of unphosphorylated Ago2, suggesting that phosphorylated Ago2 has greater stability in differentiated PC12 cells (Fig. 3C). To understand the subcellular distribution of Ago2 and miRNA, cell fractionation was done. Cellular organelles were separated on an OptiPrep density gradient by ultracentrifugation. The fractionation and subsequent analysis indicated the predominant association of Ago2 with multivesicular bodies (MVBs) and the endoplasmic reticulum (ER)/polysomes, and these results were confirmed by the distribution patterns of markers for the different organelles (Fig. 3D). The fractions enriched for MVBs and endosomes (marked by the Alix and HRS proteins) harbored more phosphorylated Ago2 than the ER-enriched fractions (marked by calnexin) of differentiated PC12 cells. A relatively larger amount of Ago2-associated let-7a miRNA was present within the endosomal fraction than in the ER fraction of nondifferentiated cells. On the other hand, a relative decrease in the amount of Ago2-associated miRNA in the endosomal fractions of differentiated PC12 cells was noted (Fig. 3E and F).

Neuronal differentiation activates the p38 signaling necessary for the phosphorylation of Ago2. How does Ago2 get phosphorylated? With the application of NGF, PC12 cells differentiate into sympathetic neuron-like cells, and this differentiation is mediated by the NGF receptor TrkA. The activated TrkA tyrosine kinase triggers signaling cascades that include the activation of the small guanine nucleotide binding protein Ras, followed by the sequential phosphorylation and activation of Raf, MEK, the ERKs (a subgroup of the MAPK superfamily), and ribosomal S6 kinases (30). NGF induces the sustained activation of classical MAPK (also known as ERK) in PC12 cells. This leads to the sustained activation of p38, a subfamily member of the MAPK superfamily, and inhibition of the p38 pathway blocks neurite outgrowth in PC12 cells. NGF treatment induces the rapid and relatively long activation of p38, and inhibition of p38 by a specific inhibitor or by expression of dominant negative constructs of the p38 pathway blocks neurite outgrowth in PC12 cells. Thus, p38 is known to have an essential role in neuronal differentiation (31). Hence, the upregulation of Ras by NGF treatment leads to p38 activation, which in turn leads to activation of its downstream kinase, MSK1, resulting in PC12 cell differentiation.

We observed an increase in phospho-p38 and phospho-mTOR levels upon differentiation of PC12 cells and SCG neurons (Fig. 4A), and this increase was reverted by application of SB203580, a specific inhibitor of p38 (Fig. 4B). In differentiated PC12 cells, inhibition of the p38 pathway by the application of SB203580 resulted in an increase in the let-7a level, let-7a activity, and Ago2-associated let-7a and a relative reduction in Ago2 Tyr phosphorylation levels (Fig. 4C to F). Consistent with our prediction of the existence of a connection between the p38 pathway, Ago2 miRNP inactivation, and PC12 cell differentiation, we also observed a reduction in PC12 cell differentiation with the application of this drug (Fig. 4G).

p38 downstream kinase MSK1 is required for Ago2 phosphorylation. Interestingly, association of phosphorylated MSK1, a downstream kinase of the p38 pathway, but not other components of the p38 pathway increased with an increase in Ago2 levels in differentiated PC12 cells. More Ago2 was also associated with immunoprecipitated p-MSK1 in differentiated PC12 cells (Fig. 5A). The total level of cellular p-MSK1 was decreased and the association of Ago2 with p-MSK1 and Ago2 phosphorylation were inhibited in differentiated PC12 cells treated with SB203580, whereas the level of total MSK1 remained unaffected (Fig. 5B). This indicates that the changes in p-MSK1 noted with neuronal differentiation were due to changes in the level of MSK1 phosphorylation and were not due to changes in its cellular level.

MSK1 is a downstream kinase of the MAPK and p38 MAPK pathways and is important in stress and mitogen-induced CREB phosphorylation in fibroblasts, PC12 cells, and embryonic stem cells (32). Inhibition of MSK1 has a negative effect on the differentiation of PC12 cells, evident by the relatively short length of neurites observed in cells treated with MSK1-specific siRNA (siMSK1) in the absence or presence of NGF in the medium (Fig. 5C). This observation was consistent with the low Ago2 level and the level of GAP43 expression in siMSK1-treated cells and was substantiated by the low level of Ago2 phosphorylation, the higher level of miRNA binding to Ago2, and the higher level of miRNA activity in cells treated with siMSK1 (Fig. 5D to F). MSK1 is a Ser-Thr kinase, and with differentiation, we detected an increase in the level of Ser phosphorylation of Ago2, as detected with a phosphorylated Ser (p-Ser)-specific antibody, in p-Ser material immunoprecipitated from differentiated PC12 cells (Fig. 5G). Conversely, immunoprecipitated Ago2 showed an increase in the p-Ser level with PC12 cell differentiation (Fig. 5H). Does p-MSK1 directly influence Ago2 phosphorylation? We incubated FLAG-HA-tagged Ago2 taken from HEK293 cells with an equal amount of p-MSK1 immunoprecipitated from undifferentiated and differentiated PC12 cells. Interestingly, only p-MSK1 from differentiated cells showed increased Tyr phosphorylation and Ser phosphorylation of FLAG-HA-tagged Ago2 (Fig. 5I), suggesting that the p-MSK1-dependent Tyr phosphorylation of Ago2 is specific for differentiated cells and it may be dependent on the Ser phosphorylation of Ago2.

A loss of miRNA let-7a activity is sufficient to cause differentiation of PC12 cells. During differentiation, the level of expression of the KRas protein increases in PC12 cells. *KRas* is required to be upregulated during the differentiation of PC12 cells and primary sympathetic neurons (1). *KRas* mRNA is a target of let-7a

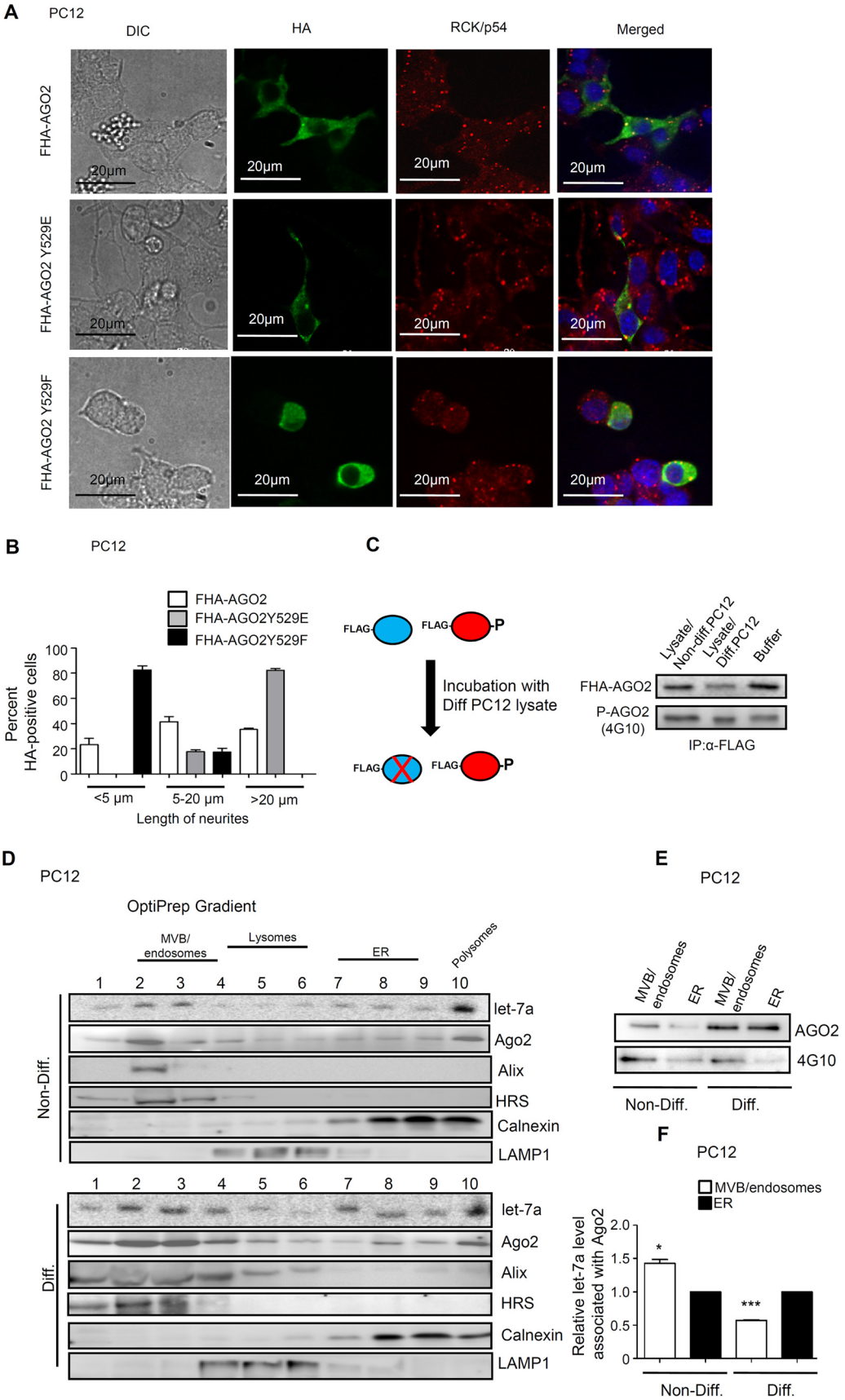

FIG 3 Phosphorylation of Ago2 is necessary for differentiation of PC12 cells. (A) Images of PC12 cells transfected with FLAG-HA (FHA)-tagged versions of Ago2 (wild type) and two different mutants, Ago2 Y529E (phosphor mimetic) and Ago2 Y529F (phosphor dead), obtained by microscopy. Transfected cells were detected by HA (green) expression, and cells were costained with Rck/p54 (red). Merged images and images obtained by differential interference contrast (DIC) are given. (B) Lengths of neurites of transfected PC12 cells. (C) Scheme of the experiment showing incubation of FLAG-tagged Ago2 purified from HEK293 cells

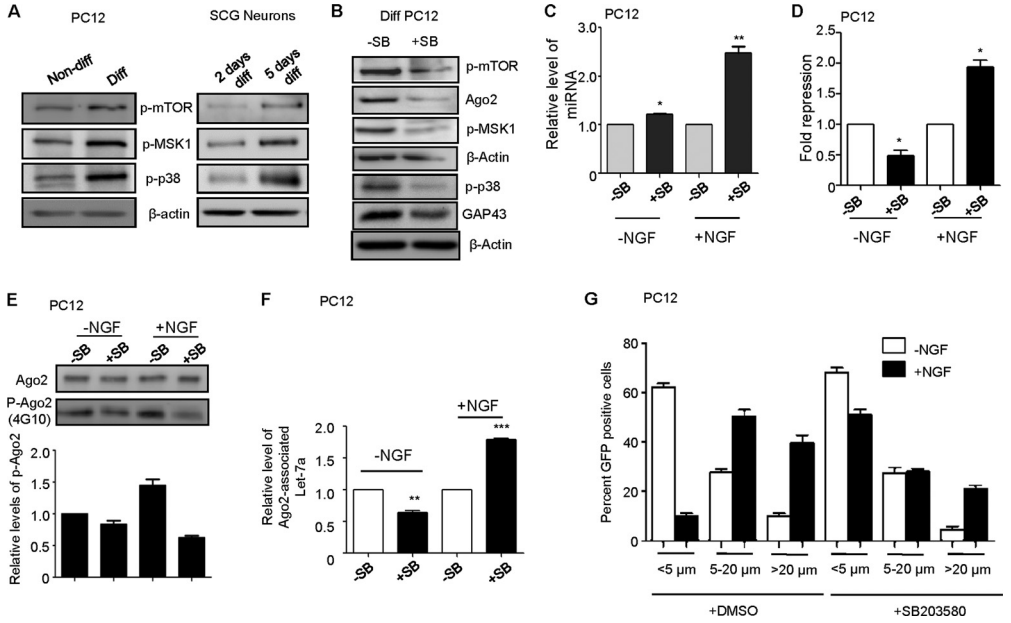

FIG 4 Neuronal differentiation activates the p38 MAPK pathway for the phosphorylation of Ago2 and inactivation of miRNPs. (A) Expression levels of phospho-mTOR (p-mTOR), phospho-p38 (p-p38), and phospho-MSK1 (p-MSK1) in undifferentiated and differentiated PC12 cells and in rat primary neurons. β-Actin was used as a loading control. (B) Effect of 16 h of treatment of differentiated PC12 cells with 1 μM SB203580 (SB), an inhibitor of the p38 signaling pathway, on the expression of Ago2, GAP43, phospho-mTOR, phospho-MSK1, and phospho-p38. β-Actin was used as a loading control. (C) Real-time PCR-based quantification of let-7a miRNA levels in undifferentiated and differentiated PC12 cells without and with application of 1 μM p38 inhibitor for 16 h. (D to F) In sets of experiments similar to those described for panel B, a luciferase assay was done to check the effect of the p38 inhibitor on let-7a activity (D), endogenous Ago2 was immunoprecipitated and 4G10 levels were checked (E, top) and quantified (E, bottom), and real-time PCR was performed to measure the relative level of immunoprecipitated Ago2-associated let-7a miRNA in PC12 cells (F). (G) Distribution of the lengths of neurites of green fluorescent protein (GFP)-positive PC12 cells upon treatment as described in the legend to panel B without and with application of the p38 inhibitor SB203580 in the absence or presence of NGF in the medium. DMSO, dimethyl sulfoxide. The data are from four biological replicates and represent means ± SEMs. *, $P < 0.05$; **, $P < 0.001$; ***, $P < 0.0001$.

miRNA, and therefore, it is possible that *KRas* activation due to the downregulation of let-7a miRNP causes the differentiation of PC12 cells. With the depletion of *KRas* by the use of siRNA against it, a lowering of the Ago2 level, along with a reduction in the level of GAP43 expression, was observed. In addition, p-MSK1 and phospho-p38 (p-p38) kinase were downregulated (Fig. 6A). KRas is also important for the differentiation of PC12 cells, as observed by statistical analysis of the length of the neurites of PC12 cells without and with *KRas* knockdown in cells treated or not treated with NGF (Fig. 6B). *KRas* is a let-7a-regulated gene that shows elevated levels of expression in lung cancer cells depleted of let-7a (29). In the experiments described above, we documented the downregulation of let-7a activity in differentiating PC12 cells. The loss of miRNA activity was coupled with the differentiation of PC12 cells. let-7a miRNA is one of the most abundant miRNAs and is known to play a central role in developmental stage switching in nematodes and also in mammalian embryonic stem cells (33, 34). Inactivation of let-7a miRNA by an anti-let-7a molecule in naive PC12 cells resulted in the increased differentiation of PC12 cells, even in the absence of exogenously added neuronal growth factors (Fig. 6C and D). The differentiation of let-7a-compromised PC12 cells was further confirmed by the elevated expression of the let-7a target (*KRas*) and the differentiation marker GAP43 in cells treated with a let-7a inhibitor (Fig. 6E). On the contrary, excess expression of the let-7a precursor, pre-let-7a, inhibited the differentiation of NGF-treated PC12 cells and reduced the length of neurites and the level of expression of the differentiation marker protein GAP43 (Fig. 6F and G). Therefore, it is likely that a reduction of let-7a miRNA activity causes the differentiation of PC12 cells and a lowering of let-7a activity is both necessary and sufficient for PC12 cell differentiation. Therefore, in a possible working model, neuronal differentiation increases the level of *KRas* expression, which subsequently enhances p38 and MSK1 phosphorylation, which induces neuronal differentiation and the further inactivation of miRNPs by phosphorylating Ago2 and

with the lysates of differentiated PC12 cells. (Left) The end product, indicating the degradation of unphosphorylated Ago2 and the stability of the phosphorylated form of Ago2. (Right) *In vitro* kinase assay with FLAG-HA-Ago2 and lysates obtained from undifferentiated and differentiated PC12 cells, along with a buffer control, to check the phosphorylated Ago2 (P-Ago2) level after a reaction detected by phospho-Tyr-specific 4G10 antibody. (D) Cell fractionation assay to detect the distribution of let-7a miRNA and Ago2 along with various organellar markers. Alix and HRS (MVB/endosome markers), LAMP1 (a lysosomal marker), and calnexin (an endoplasmic reticulum marker) were used as marker proteins. (E and F) Lighter fractions (fractions 2, 3, and 4) and heavier fractions (fractions 7, 8, and 9) of the OptiPrep density gradient were fractionated and were pooled separately, and endogenous Ago2 was immunoprecipitated to check the Tyr phosphorylation level using phosphotyrosine-specific 4G10 antibody (E) and the associated let-7a level (F). The data are from four biological replicates and represent means ± SEMs. *, $P < 0.05$; ***, $P < 0.0001$.

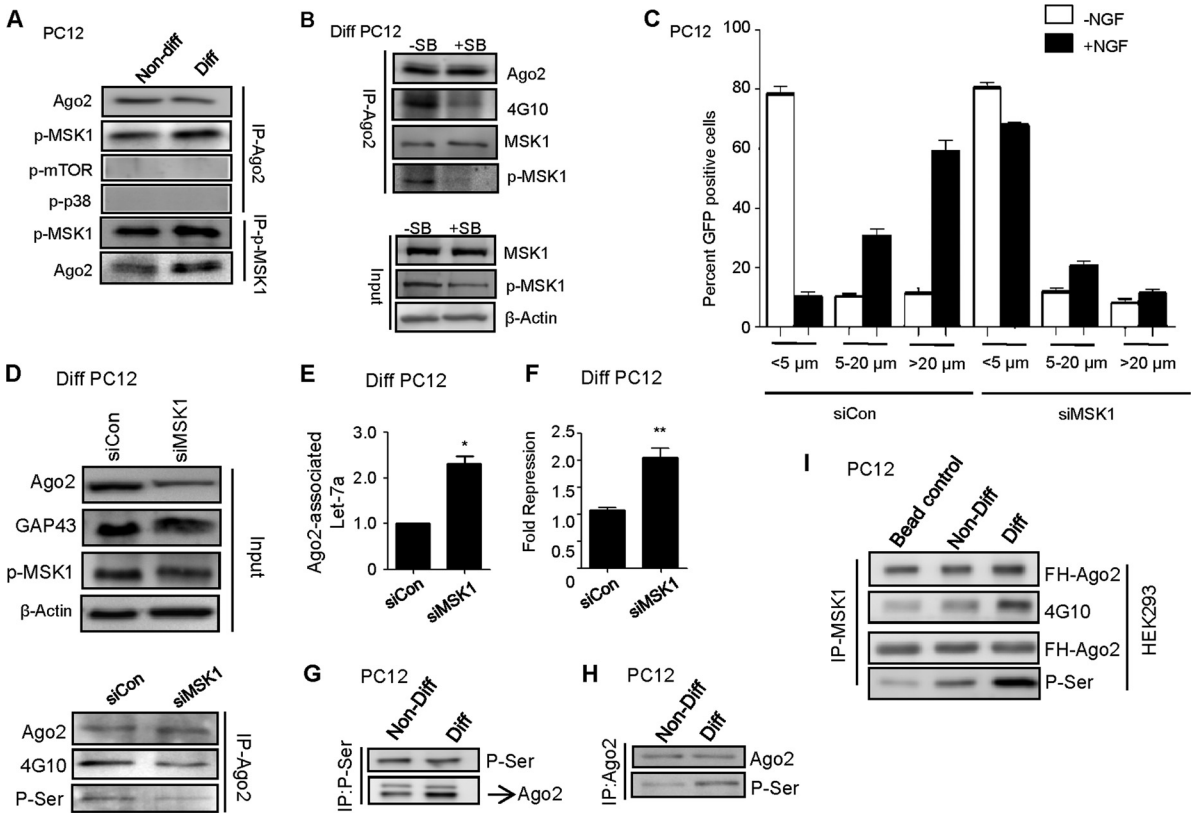

FIG 5 Involvement of p38 downstream factor MSK1 on Ago phosphorylation upon neuronal differentiation. (A) Immunoprecipitation of endogenous Ago2 from PC12 cells followed by detection of phospho-mTOR, phospho-p38, and phospho-MSK1 to find their association with Ago2 in naive and differentiated PC12 cells. Immunoprecipitation of endogenous p-MSK1 from PC12 cells followed by detection of endogenous Ago2 in naive and differentiated PC12 cells was used to document the changes in the association of p-MSK1 with Ago2 upon differentiation. (B) Immunoprecipitation of Ago2 in differentiated PC12 cells without and with application of the p38 inhibitor to detect endogenous Ago2, its phosphorylated form (as detected by the phosphotyrosine-specific 4G10 antibody), and the associated MSK1 and phospho-MSK1 by Western blotting. Input samples denote the change in the levels of MSK1 and p-MSK1 without and with the use of the p38 inhibitor SB203580. (C) Lengths of neurites of green fluorescent protein-positive PC12 cells treated with control siRNA (siCon) and siRNA against MSK1 in the absence and presence of NGF in the medium ($n = 15$ cells). (D) Western blotting to detect the effect of MSK1 knockdown by siMSK1 transfection compared to the effect of control siRNA on differentiated PC12 cells to detect changes in the levels of endogenous Ago2 and the differentiation marker GAP43. Immunoprecipitation of endogenous Ago2 from the lysates of siMSK1- and control siRNA-transfected PC12 cells was done to check the levels of tyrosine and serine phosphorylation of Ago2 by using a phosphotyrosine-specific antibody (4G10) and phosphoserine-specific antibody (P-Ser). (E) The relative level of let-7 associated with immunoprecipitated Ago2. Values were normalized to the amount of immunoprecipitated Ago2. (F) A luciferase assay was done to check the effect of siRNA-mediated MSK1 knockdown on let-7a activity compared to that of control siRNA in PC12 cells. (G) Immunoprecipitation with phosphoserine antibody to detect changes in the amount of Ser-phosphorylated Ago2 protein in naive and differentiated PC12 cells. On immunoprecipitation with phosphoserine antibody, two bands for Ago2 were observed. The lower band of 95 kDa was that of Ago2 (reconfirmed with Ago2-specific antibody) and is marked with an arrow. (H) Immunoprecipitation of Ago2 from undifferentiated and differentiated cells was done, and phosphoserine levels were detected with a specific antibody. (I) *In vitro* kinase assay with p-MSK1 isolated from PC12 cells. Lysates from undifferentiated and differentiated PC12 cells were immunoprecipitated with p-MSK1 antibody, the immunoprecipitate was incubated with an equal amount of immunologically isolated FLAG-HA-tagged Ago2 from HEK293 cells, and a kinase assay was performed. The blots indicate the change in the levels of tyrosine and serine phosphorylation of FLAG-HA-tagged Ago2 in naive and differentiated PC12 cells. The data are from four biological replicates and represent means ± SEMs. *, $P < 0.05$; **, $P < 0.001$.

subsequently induces more *KRas* activation due to the lowering of the let-7a miRNP level (Fig. 7).

DISCUSSION

The activity-induced degradation of specific miRNAs in neuronal cells was reported earlier (35). It was also noted in another report that the inactivation of specific miRNAs is required for the differentiation of fibroblasts to neurons (36). Here, we report that neuronal differentiation leads to a reduction of let-7a miRNA activity caused by uncoupling of the miRNA from Ago2.

let-7a miRNA is known to have an antiproliferative effect (37), and in neuronal stem cells, let-7a is expressed and upregulated during differentiation (38). The importance of let-7 for the differentiation of several cell lines, such as mouse neocortical cells (39) and neuronal stem cells (40), has been illustrated. Similarly, we have also observed the upregulation of let-7 miRNA with the differentiation of rat cortical neurons. However, we observed an opposite function of let-7a miRNA in the differentiation of PC12 cells. In these cells, let-7a has an antidifferentiation property, and its downregulation leads to the increased differentiation of PC12 cells. However, this is consistent with the paradoxical role of the *Ras* oncogene in the differentiation of PC12 cells (1). *Ras*, in general, has a proliferative role but is essential in the differentiation signaling pathway of PC12 cells. This could explain the paradox-

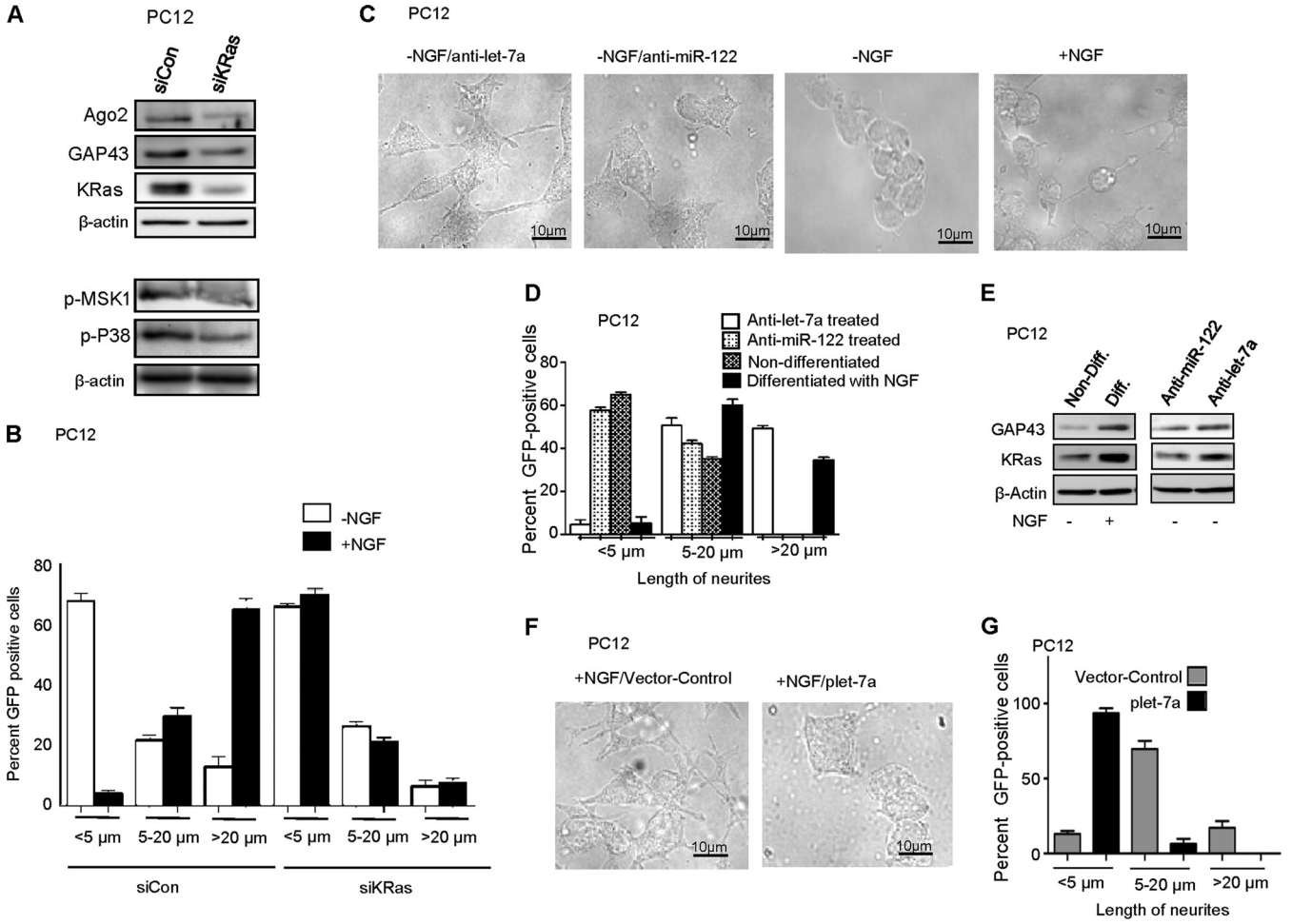

FIG 6 let-7a-mediated downregulation of *KRas* is necessary for differentiation of PC12 cells. (A) Effect of *KRas* downregulation on neuronal differentiation. PC12 cells were transfected with control siRNA and siRNA against *KRas* (siKRas), and the cells were allowed to differentiate. Western blotting was done to detect endogenous Ago2, the differentiation marker GAP43, and the signaling molecule KRas to check its downregulation. The phosphorylated forms of MSK1 and p38 were also checked. β-Actin was used as a loading control. (B) Effect of *KRas* knockdown on differentiation of PC12 cells. The lengths of neurites of green fluorescent protein-positive cells in a *KRas*-downregulated background were measured in the absence and presence of NGF in the medium. A similar measurement was done with control siRNA-transfected cells. (C and D) Differentiation status of cells treated with anti-let-7a or anti-miR-122 compared to that of undifferentiated and NGF-differentiated green fluorescent protein-positive cells ($n = 20$ cells). (C) Images of representative cells obtained by differential inference contrast. (D) Distribution of cells depending on their neurite length ($n = 20$ cells). (E) Effect of differentiation or anti-miRNA treatment on expression of *KRas* and the differentiation marker GAP43 determined by Western blotting. β-Actin was used as a loading control. (F and G) Effect of pre-let-7a expression on PC12 cells undergoing differentiation. PC12 cells grown in low-serum medium with NGF were cotransfected either with a control vector or with a pre-let-7a expression plasmid along with a green fluorescent protein expression vector. (F) Images of representative cells obtained by differential interference contrast (DIC). (G) The distribution of transfected cells (green fluorescent protein positive) on the basis of their neurite length in control or pre-let-7a-expressing PC12 cells ($n = 20$ cells). The data are from three biological replicates.

ical role of let-7a in the differentiation of sympathetic neurons, as *Ras* is a well-known target of let-7a miRNA. A recent paper reported that inhibition of let-7a miRNAs increased the level of NGF secretion by primary cultured Schwann cells and enhanced axonal outgrowth from a coculture of primary stem cells and dorsal root ganglion neurons. In addition, some members of the let-7 family are predicted to target NGF (41). An earlier report (42) also indicated a similar mechanism, in which brain-derived neurotrophic factor (BDNF) rapidly increased the Lin28 level in hippocampal neurons, causing a selective loss of Lin28-regulated miRNAs and a corresponding upregulation of translation of their target mRNAs. These observations correlate with our finding that inhibition of let-7a activity leads to the differentiation of mammalian sympathetic neurons.

It seems that the inactivation of let-7a miRNPs is sufficient for the differentiation of PC12 cells and sympathetic neurons. Expression of *KRas*, a let-7a miRNA-targeted gene, is known to play an important role in the differentiation of PC12 cells. Therefore, let-7a inactivation induces sympathetic neurons to differentiate via *KRas* upregulation, which leads to the transcriptional activation of NGF and the differentiation of sympathetic neurons and PC12 cells. It may be important to identify the other targets that let-7a and NGF reciprocally regulate in differentiating neurons.

MSK1 is a downstream kinase of the MAPK and p38 MAPK pathways, is important in stress and mitogen-treated cells, and induces CREB phosphorylation in fibroblasts, PC12 cells, and embryonic stem cells (32). Argonaute proteins bind miRNAs and repress miRNA target genes. It has already been documented that

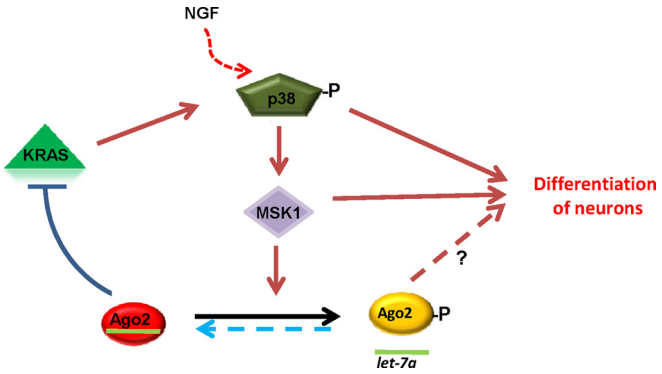

FIG 7 Mechanism of let-7a deactivation and its coupling with differentiation of neuronal cells. KRas is known to be involved in the PC12 differentiation pathway. *KRas* is a let-7a-regulated mRNA. Uncoupling of let-7a from Ago2 causes a loss of activity, and the KRas level increases with increasing time of differentiation. The uncoupling of miRNA from Ago2 is caused by its phosphorylation via the p38 MAPK/p-MSK1 pathway. Thus, Ago2 gets phosphorylated via a p-MSK1-driven pathway and let-7a activity decreases, leading to the upregulation of *KRas*, which ensures the continuous activity of the p38 MAPK pathway and the differentiation of sympathetic neurons.

human Argonaute proteins are phosphorylated at different amino acid sites. Phosphorylation of a specific tyrosine residue, Y529, prevents docking of the 5′-phosphate of small RNA and thus acts as a molecular switch that regulates small RNA binding to Argonaute proteins (21, 26). We observed that differentiation leads to the phosphorylation and activation of the serine kinase MSK1. Phosphorylation of a serine residue in Ago2 might have a role in the phosphorylation of Y529 and the consequent loss of miRNA binding. It is also possible that Y529 phosphorylation is independent of the serine phosphorylation of Ago2, as pointed out earlier (26). The exact mechanism and the subcellular site of Ago2 phosphorylation are unknown. It is also unclear how MSK1-mediated serine phosphorylation leads to the Y529 phosphorylation of the Argonaute protein.

It is possible that the miRNA-uncoupled Ago2 has a different role to play in differentiating sympathetic neurons. It is also possible that the deactivation of miRNP allows the packaging of uncoupled miRNA and phosphorylated Ago2 into P bodies independently, before they are cotransported to the distal end of neurites, where functional miRNPs may re-form upon Ago2 dephosphorylation by a putative phosphatase locally. These newly formed miRNPs may repress the target mRNAs required for growth cone formation in differentiating neurons. This may have similarities with the reversible phosphorylation-dephosphorylation of Ago2 during macrophage activation that allows the inactivation of miRNA activity in a regulated manner during the macrophage activation process and that is necessary for the proinflammatory response (26).

Experiments with phosphor-dead and phosphor-mimetic mutants of Ago2 have confirmed the importance of Ago2 phosphorylation and the consequent miRNA unbinding of Ago2 during neuronal differentiation. The phosphor-dead mutant that could not lose miRNA due to a mutation at position 529 failed to induce differentiation in PC12 cells expressing this mutant form. The predominant localization of phosphorylated Ago2 and uncoupled miRNA in the late endosome/MVB fraction raised a question about the fate of the uncoupled miRNAs. Whether miRNAs are packaged inside vesicles that are destined to become exosomes and either exported or transported to the other end of the cell is a pertinent question. Similarly, whether the phosphorylated Ago2 found to be localized with late endosomes/MVBs is targeted to lysosomes and degraded is another unanswered question. It may be noted that a similar observation has also been reported for lipopolysaccharide (LPS)-treated macrophages, where the phosphorylation of Ago2 ensured the activation of macrophages (26).

Thus, our report highlights a mechanism by which Ago2-associated miRNA let-7a is uncoupled upon p-MSK1-induced phosphorylation of Ago2 and thereby leads to the upregulation of KRas, a molecule involved in neuronal differentiation.

ACKNOWLEDGMENTS

We acknowledge Witold Filipowicz, Gunter Meister, and Edouard Bertrand for different plasmid constructs and also for valuable discussions.

S.N.B. was supported by The Wellcome Trust International Senior Research Fellowship (ISRF), while S.P. received support from CSIR. We are supported by the Wellcome Trust ISRF fund and CSIR Network Project Fund MinD (BSC0115).

FUNDING INFORMATION

Wellcome Trust provided funding under grant number 084324/Z/07/A, and Council of Scientific and Industrial Research (CSIR) provided funding under grant number BSC0115 to Suvendra Nath Bhattacharyya.

REFERENCES

1. **Vaudry D, Stork PJ, Lazarovici P, Eiden LE.** 2002. Signaling pathways for PC12 cell differentiation: making the right connections. Science **296:** 1648–1649. http://dx.doi.org/10.1126/science.1071552.
2. **Greene LA, Tischler AS.** 1976. Establishment of a noradrenergic clonal line of rat adrenal pheochromocytoma cells which respond to nerve growth factor. Proc Natl Acad Sci U S A **73:**2424–2428. http://dx.doi.org/10.1073/pnas.73.7.2424.
3. **Dichter MA, Tischler AS, Greene LA.** 1977. Nerve growth factor-induced increase in electrical excitability and acetylcholine sensitivity of a rat pheochromocytoma cell line. Nature **268:**501–504. http://dx.doi.org/10.1038/268501a0.
4. **Jeon CY, Jin JK, Koh YH, Chun W, Choi IG, Kown HJ, Kim YS, Park JB.** 2010. Neurites from PC12 cells are connected to each other by synapse-like structures. Synapse **64:**765–772. http://dx.doi.org/10.1002/syn.20789.
5. **D'Arcangelo G, Halegoua S.** 1993. A branched signaling pathway for nerve growth factor is revealed by Src-, Ras-, and Raf-mediated gene inductions. Mol Cell Biol **13:**3146–3155. http://dx.doi.org/10.1128/MCB.13.6.3146.
6. **Bhattacharyya SN, Habermacher R, Martine U, Closs EI, Filipowicz W.** 2006. Relief of microRNA-mediated translational repression in human cells subjected to stress. Cell **125:**1111–1124. http://dx.doi.org/10.1016/j.cell.2006.04.031.
7. **Jakymiw A, Lian S, Eystathioy T, Li S, Satoh M, Hamel JC, Fritzler MJ, Chan EK.** 2005. Disruption of GW bodies impairs mammalian RNA interference. Nat Cell Biol **7:**1267–1274. http://dx.doi.org/10.1038/ncb1334.
8. **Pillai RS, Bhattacharyya SN, Artus CG, Zoller T, Cougot N, Basyuk E, Bertrand E, Filipowicz W.** 2005. Inhibition of translational initiation by let-7 microRNA in human cells. Science **309:**1573–1576. http://dx.doi.org/10.1126/science.1115079.
9. **Vreugdenhil E, Berezikov E.** 2010. Fine-tuning the brain: microRNAs. Front Neuroendocrinol **31:**128–133. http://dx.doi.org/10.1016/j.yfrne.2009.08.001.
10. **Miska EA, Alvarez-Saavedra E, Townsend M, Yoshii A, Sestan N, Rakic P, Constantine-Paton M, Horvitz HR.** 2004. Microarray analysis of microRNA expression in the developing mammalian brain. Genome Biol **5:**R68. http://dx.doi.org/10.1186/gb-2004-5-9-r68.
11. **Krichevsky AM, Sonntag KC, Isacson O, Kosik KS.** 2006. Specific microRNAs modulate embryonic stem cell-derived neurogenesis. Stem Cells **24:**857–864. http://dx.doi.org/10.1634/stemcells.2005-0441.

12. **Rajasethupathy P, Fiumara F, Sheridan R, Betel D, Puthanveettil SV, Russo JJ, Sander C, Tuschl T, Kandel E.** 2009. Characterization of small RNAs in Aplysia reveals a role for miR-124 in constraining synaptic plasticity through CREB. Neuron **63:**803–817. http://dx.doi.org/10.1016/j.neuron.2009.05.029.
13. **Yu JY, Chung KH, Deo M, Thompson RC, Turner DL.** 2008. MicroRNA miR-124 regulates neurite outgrowth during neuronal differentiation. Exp Cell Res **314:**2618–2633. http://dx.doi.org/10.1016/j.yexcr.2008.06.002.
14. **Edbauer D, Neilson JR, Foster KA, Wang CF, Seeburg DP, Batterton MN, Tada T, Dolan BM, Sharp PA, Sheng M.** 2010. Regulation of synaptic structure and function by FMRP-associated microRNAs miR-125b and miR-132. Neuron **65:**373–384. http://dx.doi.org/10.1016/j.neuron.2010.01.005.
15. **Magill ST, Cambronne XA, Luikart BW, Lioy DT, Leighton BH, Westbrook GL, Mandel G, Goodman RH.** 2010. microRNA-132 regulates dendritic growth and arborization of newborn neurons in the adult hippocampus. Proc Natl Acad Sci U S A **107:**20382–20387. http://dx.doi.org/10.1073/pnas.1015691107.
16. **Bruno IG, Karam R, Huang L, Bhardwaj A, Lou CH, Shum EY, Song HW, Corbett MA, Gifford WD, Gecz J, Pfaff SL, Wilkinson MF.** 2011. Identification of a microRNA that activates gene expression by repressing nonsense-mediated RNA decay. Mol Cell **42:**500–510. http://dx.doi.org/10.1016/j.molcel.2011.04.018.
17. **Friedman RC, Farh KK, Burge CB, Bartel DP.** 2009. Most mammalian mRNAs are conserved targets of microRNAs. Genome Res **19:**92–105. http://dx.doi.org/10.1101/gr.082701.108.
18. **Qi HH, Ongusaha PP, Myllyharju J, Cheng D, Pakkanen O, Shi Y, Lee SW, Peng J, Shi Y.** 2008. Prolyl 4-hydroxylation regulates Argonaute 2 stability. Nature **455:**421–424. http://dx.doi.org/10.1038/nature07186.
19. **Kirino Y, Kim N, de Planell-Saguer M, Khandros E, Chiorean S, Klein PS, Rigoutsos I, Jongens TA, Mourelatos Z.** 2009. Arginine methylation of Piwi proteins catalysed by dPRMT5 is required for Ago3 and Aub stability. Nat Cell Biol **11:**652–658. http://dx.doi.org/10.1038/ncb1872.
20. **Horman SR, Janas MM, Litterst C, Wang B, MacRae IJ, Sever MJ, Morrissey DV, Graves P, Luo B, Umesalma S, Qi HH, Miraglia LJ, Novina CD, Orth AP.** 2013. Akt-mediated phosphorylation of Argonaute 2 downregulates cleavage and upregulates translational repression of microRNA targets. Mol Cell **50:**356–367. http://dx.doi.org/10.1016/j.molcel.2013.03.015.
21. **Rudel S, Wang Y, Lenobel R, Korner R, Hsiao HH, Urlaub H, Patel D, Meister G.** 2011. Phosphorylation of human Argonaute proteins affects small RNA binding. Nucleic Acids Res **39:**2330–2343. http://dx.doi.org/10.1093/nar/gkq1032.
22. **Shen J, Xia W, Khotskaya YB, Huo L, Nakanishi K, Lim SO, Du Y, Wang Y, Chang WC, Chen CH, Hsu JL, Wu Y, Lam YC, James BP, Liu X, Liu CG, Patel DJ, Hung MC.** 2013. EGFR modulates microRNA maturation in response to hypoxia through phosphorylation of AGO2. Nature **497:**383–387. http://dx.doi.org/10.1038/nature12080.
23. **Zeng Y, Sankala H, Zhang X, Graves PR.** 2008. Phosphorylation of Argonaute 2 at serine-387 facilitates its localization to processing bodies. Biochem J **413:**429–436. http://dx.doi.org/10.1042/BJ20080599.
24. **Liu J, Carmell MA, Rivas FV, Marsden CG, Thomson JM, Song JJ, Hammond SM, Joshua-Tor L, Hannon GJ.** 2004. Argonaute2 is the catalytic engine of mammalian RNAi. Science **305:**1437–1441. http://dx.doi.org/10.1126/science.1102513.
25. **Lopez-Orozco J, Pare JM, Holme AL, Chaulk SG, Fahlman RP, Hobman TC.** 2015. Functional analyses of phosphorylation events in human Argonaute 2. RNA **21:**2030–2038. http://dx.doi.org/10.1261/rna.053207.115.
26. **Mazumder A, Bose M, Chakraborty A, Chakrabarti S, Bhattacharyya SN.** 2013. A transient reversal of miRNA-mediated repression controls macrophage activation. EMBO Rep **14:**1008–1016. http://dx.doi.org/10.1038/embor.2013.149.
27. **Barancik M, Bohacova V, Kvackajova J, Hudecova S, Krizanova O, Breier A.** 2001. SB203580, a specific inhibitor of p38-MAPK pathway, is a new reversal agent of P-glycoprotein-mediated multidrug resistance. Eur J Pharm Sci **14:**29–36. http://dx.doi.org/10.1016/S0928-0987(01)00139-7.
28. **Zareen N, Greene LA.** 2009. Protocol for culturing sympathetic neurons from rat superior cervical ganglia (SCG). J Vis Exp **2009:**988. http://dx.doi.org/10.3791/988.
29. **Johnson SM, Grosshans H, Shingara J, Byrom M, Jarvis R, Cheng A, Labourier E, Reinert KL, Brown D, Slack FJ.** 2005. RAS is regulated by the let-7 microRNA family. Cell **120:**635–647. http://dx.doi.org/10.1016/j.cell.2005.01.014.
30. **Xing J, Kornhauser JM, Xia Z, Thiele EA, Greenberg ME.** 1998. Nerve growth factor activates extracellular signal-regulated kinase and p38 mitogen-activated protein kinase pathways to stimulate CREB serine 133 phosphorylation. Mol Cell Biol **18:**1946–1955. http://dx.doi.org/10.1128/MCB.18.4.1946.
31. **Morooka T, Nishida E.** 1998. Requirement of p38 mitogen-activated protein kinase for neuronal differentiation in PC12 cells. J Biol Chem **273:**24285–24288. http://dx.doi.org/10.1074/jbc.273.38.24285.
32. **Zheng WH, Quirion R.** 2006. Insulin-like growth factor-1 (IGF-1) induces the activation/phosphorylation of Akt kinase and cAMP response element-binding protein (CREB) by activating different signaling pathways in PC12 cells. BMC Neurosci **7:**51. http://dx.doi.org/10.1186/1471-2202-7-51.
33. **Bussing I, Slack FJ, Grosshans H.** 2008. let-7 microRNAs in development, stem cells and cancer. Trends Mol Med **14:**400–409. http://dx.doi.org/10.1016/j.molmed.2008.07.001.
34. **Reinhart BJ, Slack FJ, Basson M, Pasquinelli AE, Bettinger JC, Rougvie AE, Horvitz HR, Ruvkun G.** 2000. The 21-nucleotide let-7 RNA regulates developmental timing in Caenorhabditis elegans. Nature **403:**901–906. http://dx.doi.org/10.1038/35002607.
35. **Krol J, Busskamp V, Markiewicz I, Stadler MB, Ribi S, Richter J, Duebel J, Bicker S, Fehling HJ, Schubeler D, Oertner TG, Schratt G, Bibel M, Roska B, Filipowicz W.** 2010. Characterizing light-regulated retinal microRNAs reveals rapid turnover as a common property of neuronal microRNAs. Cell **141:**618–631. http://dx.doi.org/10.1016/j.cell.2010.03.039.
36. **Xue Y, Ouyang K, Huang J, Zhou Y, Ouyang H, Li H, Wang G, Wu Q, Wei C, Bi Y, Jiang L, Cai Z, Sun H, Zhang K, Zhang Y, Chen J, Fu XD.** 2013. Direct conversion of fibroblasts to neurons by reprogramming PTB-regulated microRNA circuits. Cell **152:**82–96. http://dx.doi.org/10.1016/j.cell.2012.11.045.
37. **Peng Y, Laser J, Shi G, Mittal K, Melamed J, Lee P, Wei JJ.** 2008. Antiproliferative effects by let-7 repression of high-mobility group A2 in uterine leiomyoma. Mol Cancer Res **6:**663–673. http://dx.doi.org/10.1158/1541-7786.MCR-07-0370.
38. **Rybak A, Fuchs H, Smirnova L, Brandt C, Pohl EE, Nitsch R, Wulczyn FG.** 2008. A feedback loop comprising lin-28 and let-7 controls pre-let-7 maturation during neural stem-cell commitment. Nat Cell Biol **10:**987–993. http://dx.doi.org/10.1038/ncb1759.
39. **Schwamborn JC, Berezikov E, Knoblich JA.** 2009. The TRIM-NHL protein TRIM32 activates microRNAs and prevents self-renewal in mouse neural progenitors. Cell **136:**913–925. http://dx.doi.org/10.1016/j.cell.2008.12.024.
40. **Nicklas S, Okawa S, Hillje AL, Gonzalez-Cano L, Del Sol A, Schwamborn JC.** 2015. The RNA helicase DDX6 regulates cell-fate specification in neural stem cells via miRNAs. Nucleic Acids Res **43:**2638–2654. http://dx.doi.org/10.1093/nar/gkv138.
41. **Li S, Wang X, Gu Y, Chen C, Wang Y, Liu J, Hu W, Yu B, Ding F, Liu Y, Gu X.** 2015. Let-7 microRNAs regenerate peripheral nerve regeneration by targeting nerve growth factor. Mol Ther **23:**423–433. http://dx.doi.org/10.1038/mt.2014.220.
42. **Huang YW, Ruiz CR, Eyler EC, Lin K, Meffert MK.** 2012. Dual regulation of miRNA biogenesis generates target specificity in neurotrophin-induced protein synthesis. Cell **148:**933–946. http://dx.doi.org/10.1016/j.cell.2012.01.036.